Acoustically Controlled Spin Precession Revealed by Two-dimensional Imaging of Spin Transport in GaAs

Haruki Sanada†, *Hideki Gotoh, Koji Onomitsu, and Tetsuomi Sogawa*

Abstract

Magneto-optic Kerr microscopy was used to investigate the spin precession of electrons traveling in semiconductor quantum wells by using surface acoustic waves (SAWs). Two-dimensional images of the SAW-induced spin flow reveal anisotropic spin precession behavior caused by the coexistence of different types of spin-orbit interactions. The dependence of spin-orbit effective magnetic fields on SAW intensity indicates the existence of acoustically controllable spin-orbit interactions resulting from SAW-induced strain and SAW-induced Rashba contributions. These phenomena will provide the versatility needed for spin manipulation in future spintronic applications such as spin transistors and quantum computers.

1. Introduction

In conventional semiconductor electronics, electron spins have been ignored because they are randomly oriented and cancel out completely. The research field called *semiconductor spintronics* aims to extract spin properties in order to use them for both classical and quantum information technologies, which will achieve higher processing speeds, lower electrical power consumption, and higher integration densities than conventional charge-based devices [1]. Understanding the spin dynamics of electrons moving in semiconductors is one of the keys to developing spintronic technologies because it will enable electrical spin manipulation without external magnetic fields in ways that have been proposed for spin field-effect transistors [2], spin filters [3], and quantum computers [4]. In a system lacking inversion symmetry, moving electrons feel effective magnetic fields even in the absence of real magnetic fields. This is caused by spin-orbit interactions (SOIs) arising from relativistic effects. In general, magnetic fields induce spin precession, which is the rotation of the spin angular momentum around the magnetic field. Because of this, moving spins precess with a frequency proportional to the strength of the SOIs. So far, spin transport experiments using a DC-electric field [5] have succeeded in observing the spin precessions induced by SOIs in the absence of a real magnetic field [6]. Surface acoustic waves (SAWs) applied to semiconductor quantum wells (QWs), which confine electrons in thin layers sandwiched between barrier layers made of other materials, provide another way to transport electron spins [7]–[9]. This method has the advantage of effectively suppressing the dominant spin relaxation process caused by the electron-hole exchange interaction in undoped semiconductors [10] owing to the spatial separation of electrons and holes in the type-II-like lateral potential modulation created by the SAWs [7]. As a result, it has become possible to transport electrons by using SAWs over distances of nearly 100 μm while maintaining their spin coherence during precession around the effective magnetic fields caused by SOIs [8].

Here, we used magneto-optic Kerr rotation (KR)

† NTT Basic Research Laboratories
Atsugi-shi, 243-0198 Japan

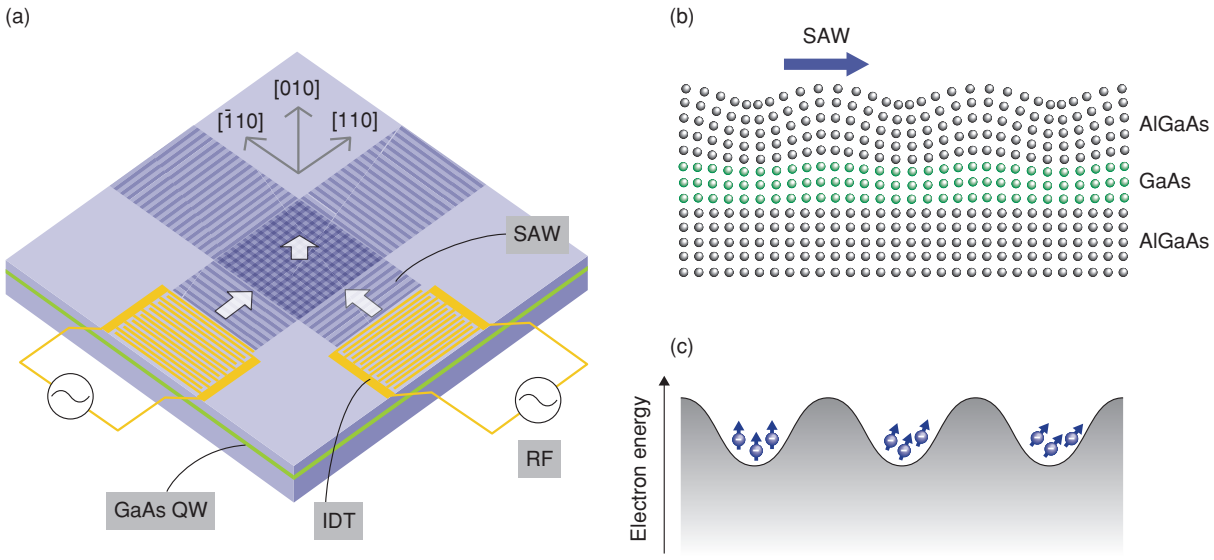

Fig. 1. (a) Schematic view of the sample. (b) SAW-induced displacement of atoms in the sample's cross section. Electrons are confined in a GaAs/AlGaAs QW. (c) Conduction band energy for the QW shown in (b). Electrons are trapped in the valleys of the modulated potential and transported by the SAWs.

microscopy to explore the two-dimensional (2D) dynamics of traveling spins under SAWs over a wide range of acoustic amplitudes. The present experiment revealed the existence of spatially anisotropic SOIs as well as their dependence on SAW strength. A theoretical analysis of the experimental results elucidated the mechanisms of the acoustically controllable spin dynamics. The phenomena will provide a new approach for the spin-manipulation as well as spin transport without the application of any magnetic fields or DC electric fields.

2. Experiment

A schematic view of the sample is shown in **Fig. 1(a)**. It was a 20-nm-thick undoped GaAs single QW with short-period GaAs/AlAs (average Al content: 30%) barriers grown by molecular-beam epitaxy on a (001) semi-insulating GaAs substrate. The QW was located 485 nm below the surface. A 50-nm-thick Al film deposited on top of the sample was processed by electron-beam lithography into interdigital transducers (IDTs), which were designed for operation at a SAW wavelength of 2.55 μm and frequency of 1.154 GHz. Rayleigh SAWs propagate along either [110] or [$\bar{1}$10], depending on the direction of the applied radio frequency (RF) signal, with a SAW velocity $|\mathbf{v}_{SAW}|$ = 2.9 km/s. The single SAW beams produce *moving wires*, which are formed by the one-dimensional (1D) lateral confinement of the SAW-induced piezoelectric potential (**Figs. 1(b)** and **(c)**). Interference between two orthogonal SAW beams forms *moving dots* traveling along [010] with a velocity of $\sqrt{2}\,|\mathbf{v}_{SAW}|$ [8], as shown in Fig. 1(a).

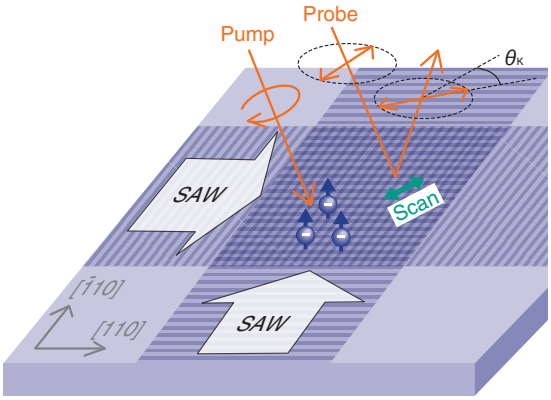

Fig. 2. Setup for spatially resolved KR measurements.

The spin dynamics during transport was measured by temporally and spatially resolved KR microscopy using a mode-locked Ti:sapphire laser (1.5 ps, 82 MHz, 1.527 eV), as illustrated in **Fig. 2**. Circularly polarized pump pulses (average power: 1.1 μW) were focused at a fixed position on the sample. Linearly polarized probe pulses (0.9 μW) with a time delay

relative to the pump pulses were scanned over the surface and the KR angle θ_K of their reflected light was measured by a balanced detection technique. The pump light's polarization was modulated between left- and right-circular polarizations at 50.1 kHz, and the probe light was chopped with an acousto-optic modulator at 52.0 kHz. The difference frequency (1.9 kHz) was used as a reference for lock-in detection. The full width at half maximum (FWHM) spot size of the normally incident probe beam was approximately 3 μm, whereas the waist size of the obliquely incident pump beam was 6 μm and its spot on the sample was slightly elongated in the [100] direction. The position of the probe light spot was scanned in the QW plane for spatially resolved KR measurements. For the 2D mapping of steady-state spin distributions, we chose to use a two-color pump-probe method using a pair of continuous-wave Ti: sapphire lasers. All the measurements were carried out at a low temperature (30 K), where long-distance spin transport is expected [7], [8] in the absence of applied magnetic fields.

3. Results and discussion

The spatiotemporal evolution of photoinjected spins trapped in moving dots traveling in the [010] direction is shown in **Fig. 3**. The slope of the KR signal indicates that the spin-polarized electrons moved with the expected velocity of $\sqrt{2}\,|\mathbf{v}_{SAW}| = 4.14$ km/s. The oscillations with a period of about 4.5 ns are attributed to spin precession around the spin-orbit effective magnetic field, as shown in the inset. The data thus clearly demonstrate that our method successfully extracted information about the spin dynamics, including spin transport and SOI-induced spin precession.

Spatial maps of steady-state spin densities for moving wires are shown in **Figs. 4(a)** and **(c)** and that for moving dots is shown in **Fig. 4(b)**. In the two-color measurement, the pump energy was fixed at 1.527 eV, whereas the probe energy was tuned to 1.525, 1.526, and 1.528 eV for [$\bar{1}$10], [010], and [110], respectively, because the bandgap energies at the electron-trapping positions were modulated by SAW fields [11]. The pump (probe) power was 20 (0.9) μW. In contrast to the well-confined carrier transport achieved by moving dots (Fig. 4(b)), carriers in moving wires diffused rapidly along the wire axis (Figs. 4(a) and (c)). Although the KR signal for the wires was reduced by the carrier diffusion, we could access the momentum direction dependences of spin precessions (**Fig. 4(d)**),

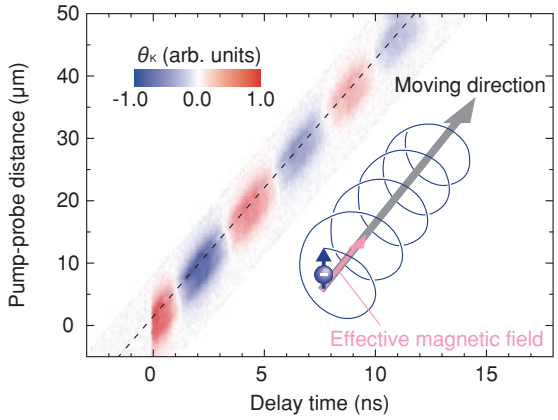

Fig. 3. Spatiotemporal evolution of the KR signal for moving dots traveling along [010]. The dashed line shows the slope determined from the estimated velocity of the moving dots. The inset shows the motion of the spin precessing around the effective magnetic field during transport.

where the sum of the mapping data (Figs. 4(a)–(c)) shows that the isophase lines have clear elliptical shapes. In **Fig. 4(e)**, the KR angles θ_K (open circles) along particular axes ([110], [010], and [$\bar{1}$10]) are fitted with a function $\theta_K(d)=\theta_0 \cos(2\pi\kappa d)\exp(-d/L_s)$, where d is the pump-probe distance and L_s and κ are fitting parameters representing the spin decay length and spatial precession frequency, respectively. We obtained $\kappa_{[110]} = 0.0589 \pm 0.0008$, $\kappa_{[010]} = 0.05369 \pm 0.00009$, and $\kappa_{[\bar{1}10]} = 0.0460 \pm 0.0006$ μm^{-1} for the traveling directions [110], [010], and [$\bar{1}$10], respectively. Since κ is proportional to the spin-orbit effective magnetic field, these results demonstrate that the SOIs are spatially anisotropic in the present system.

The SOI dependence on the traveling direction is caused by the coexistence of different types of SOIs [6], [12]–[14]. For electrons confined in (001) QWs, the momentum-dependent effective magnetic field $\Omega_{so}(\mathbf{k})$is primarily determined by k-linear terms, which are classified into two types [15]:

$$\Omega^{\alpha}(\mathbf{k})=\frac{2\alpha}{\hbar}\begin{bmatrix} k_Y \\ -k_X \\ 0 \end{bmatrix},\quad \Omega^{\beta}(\mathbf{k})=\frac{2\beta}{\hbar}\begin{bmatrix} -k_X \\ k_Y \\ 0 \end{bmatrix}, \qquad (1)$$

where we used a coordinate system with base vectors $\hat{\mathbf{X}}$ // [100], $\hat{\mathbf{Y}}$ // [010], and $\hat{\mathbf{Z}}$ // [001]. The orientation dependences of $\Omega^{\alpha}(\mathbf{k})$ and $\Omega^{\beta}(\mathbf{k})$ in $\mathbf{k}$ space are shown in **Fig. 5**. Since these vectors have different dependences on the direction of $\mathbf{k}$, their coexistence

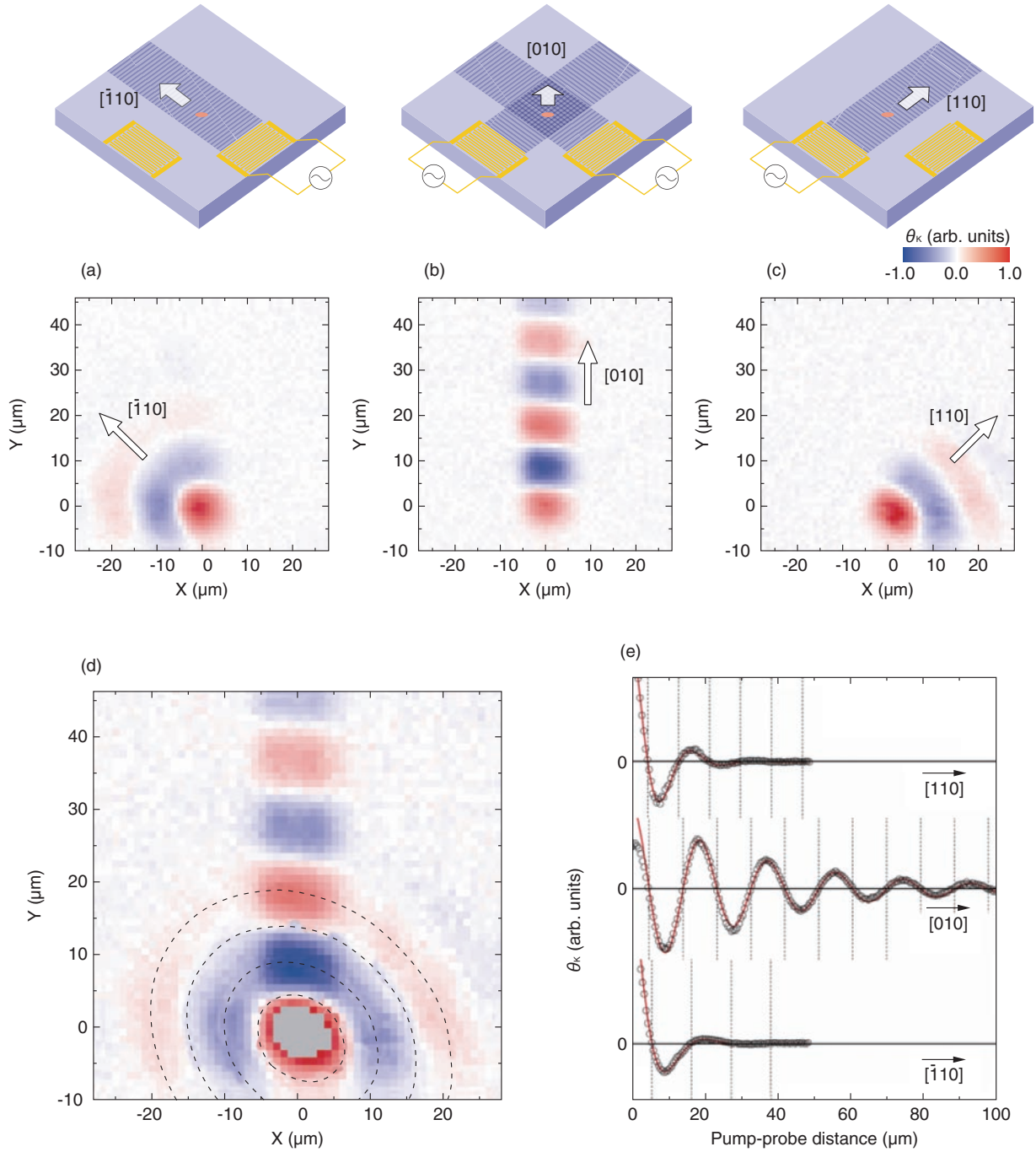

Fig. 4. (a)–(d) 2D images of spin densities for moving wires traveling along [$\bar{1}$10] (a) and [110] (c) and for moving dots traveling along [010] (b). The sum of the data (a)–(c) is plotted in (d), where the dashed ellipses are guides for the eye. (e) Kerr rotation signals along the three directions in the data (a)–(c) are plotted (black open circles) and the red lines are fitting curves. The dashed lines represent precession phases of π/2, (3/2)π, (5/2)π, ...

leads to twofold symmetry of $|\Omega^{total}(\mathbf{k})|=|\Omega^{\alpha}(\mathbf{k})+\Omega^{\beta}(\mathbf{k})|$, as illustrated in Fig. 5. In general, $\Omega^{\alpha}(\mathbf{k})$ and $\Omega^{\beta}(\mathbf{k})$ are mainly induced by the structural inversion asymmetry caused by a static electric field (Rashba SOI [16]) and the intrinsic bulk inversion asymmetry (Dresselhaus SOI [17]), respectively. In addition to

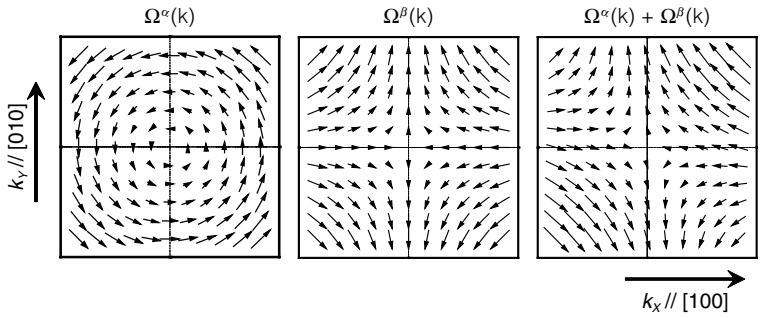

Fig. 5. Effective magnetic fields $\mathbf{\Omega}^{\alpha}$, $\mathbf{\Omega}^{\beta}$, and $\mathbf{\Omega}^{\alpha} + \mathbf{\Omega}^{\beta}$ plotted as vectors in **k** space. $\alpha < 0$, $\beta > 0$, and $\beta > |\alpha|$ are assumed in this figure.

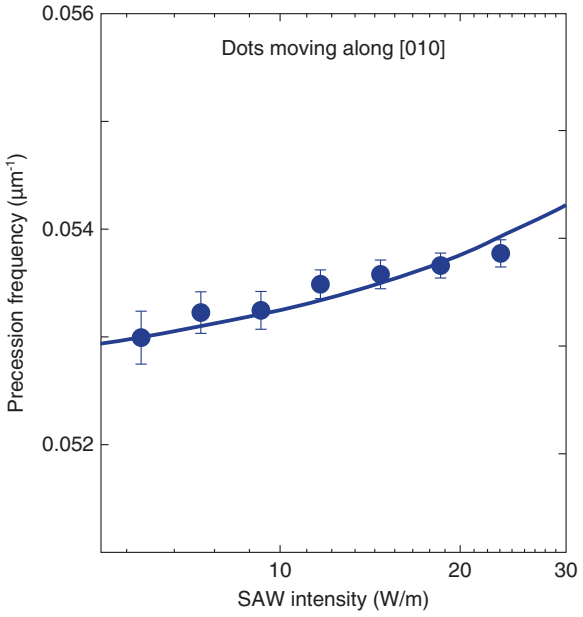

Fig. 6. SAW intensity dependence of precession frequency for moving dots. The solid line was obtained by calculation. The error bars for the data represent two standard errors of the parameters obtained from a least-squares fitting.

these static contributions, the present system should have a dynamic Rashba SOI induced by the vertical component of the SAW piezoelectric field as well as strain-induced SOIs [18]–[20].

As expected, the precession frequency varied with the SAW intensity, which is defined as the acoustic power flux per unit length along a cross-section of the SAW beam. The symbols in **Fig. 6** represent the experimentally obtained precession frequency as a function of the SAW intensity for moving dots. We estimated the SAW intensities from the bandgap shift observed in photoluminescence spectra [21]. As the SAW intensity increased, the precession frequency increased monotonically, suggesting that the SOI is acoustically controllable. The experimental data were well reproduced by simulating the precession frequency (solid lines in Fig. 6) [22], where each SOI contribution to the spin precessions was estimated from the calculation of the Rayleigh SAW fields including the piezoelectric coupling [23]. This analysis revealed the contributions of SAW-dependent Rashba and strain SOIs to the total SOI, indicating that the spin rotation angle can be tuned by adjusting the SAW intensity.

4. Conclusion

We studied the SOIs of electrons traveling in semiconductor QWs by using SAW fields. The temporally and/or spatially resolved KR technique enabled 2D imaging of the traveling spins, which revealed anisotropic spin precession behavior resulting from the coexistence of different types of SOIs. The dependence of the precession frequencies on SAW intensity, which was analyzed on the basis of a theoretical model, indicates that the strengths of the SOIs due to strain and Rashba contributions can be tuned by adjusting the SAW intensity. Our experimental results will be beneficial for further investigation of acoustically induced SOIs in semiconductors. They will also provide the versatility needed for spin manipulation via dynamically controlled SOIs in future spintronic applications such as spin transistors and quantum computers.

Acknowledgments

We thank P. V. Santos of Paul-Drude-Institut für Festkörperelektronik, Berlin, Germany, and J. Nitta and M. Kohda of Department of Materials Science, Tohoku University, Sendai, Japan, for useful discussions. This work was partly supported by the Japan Society for the Promotion of Science (JSPS).

References

[1] S. A. Wolf, D. D. Awschalom, R. A. Buhrman, J. M. Daughton, S. von Molnár, M. L. Roukes, A. Y. Chtchelkanova, and D. M. Treger, "Spintronics: A Spin-based Electronics Vision for the Future," Science, Vol. 294, pp. 1488–1495, 2001.

[2] S. Datta and B. Das, "Electronic Analog of the Electro-optic Modulator," Appl. Phys. Lett., Vol. 56, No. 7, p. 665, 1990.

[3] T. Koga and S. Datta, "Spin-filter Device Based on the Rashba Effect Using a Nonmagnetic Resonant Tunneling Diode," Phys. Rev. Lett., Vol. 88, No. 12, p. 126601, 2002; J. Ohe, M. Yamamoto, T. Ohtsuki, and J. Nitta, "Mesoscopic Stern-Gerlach Spin Filter by Nonuniform Spin-orbit Interaction," Phys. Rev. B, Vol. 72, No. 12, p. 041308, 2005.

[4] D. Stepanenko and N. E. Bonesteel, "Universal Quantum Computation through Control of Spin-orbit Coupling," Phys. Rev. Lett., Vol. 93, No. 14, p. 140501, 2004.

[5] J. M. Kikkawa and D. D. Awschalom, "Lateral Drag of Spin Coherence in Gallium Arsenide," Nature (London) Vol. 397, No. 6715, p. 139, 1999; D. Hägele, M. Oestreich, W. W. Rühle, N. Nestle, and K. Eberl, "Spin Transport in GaAs," Appl. Phys. Lett., Vol. 73, No. 11, p. 1580, 1998; H. Sanada, I. Arata, Y. Ohno, Z. Chen, K. Kayanuma, Y. Oka, F. Matsukura, and H. Ohno, "Relaxation of Photoinjected Spins during Drift Transport in GaAs," Appl. Phys. Lett., Vol. 81, No. 15, p. 2788, 2002.

[6] Y. Kato, R. C. Myers, A. C. Gossard, and D. D. Awschalom, "Coherent Spin Manipulation without Magnetic Fields in Strained Semiconductors," Nature (London), Vol. 427, No. 6969, p. 50, 2004.

[7] T. Sogawa, P. V. Santos, S. K. Zhang, S. Eshlaghi, A. D. Wieck, and K. H. Ploog, "Transport and Lifetime Enhancement of Photoexcited Spins in GaAs by Surface Acoustic Waves," Phys. Rev. Lett., Vol. 87, No. 27, p. 276601, 2001.

[8] J. A. H. Stotz, R. Hey, P. V. Santos, and K. H. Ploog, "Coherent Spin Transport through Dynamic Quantum Dots," Nature Mater., Vol. 4, No. 8, p. 585, 2005.

[9] O. D. D. Couto, Jr., F. Iikawa, J. Rudolph, R. Hey, and P. V. Santos, "Anisotropic Spin Transport in (110) GaAs Quantum Wells," Phys. Rev. Lett., Vol. 98, No. 3, p. 036603, 2007.

[10] G. L. Bir, A. G. Aronov, and G. E. Pikus, "Spin Relaxation of Electrons due to Scattering by Holes," Zh. Eksp. Teor. Fiz. Vol. 69, No. 4, p. 1382, 1975 [Sov. Phys. JETP, Vol. 42, p. 705, 1975].

[11] F. Alsina, P.V. Santos, and R. Hey, "Spatial-dispersion-induced Acoustic Anisotropy in Semiconductor Structures," Phys. Rev. B, Vol. 65, No. 19, p. 193301, 2002.

[12] L. Meier, G. Salis, I. Shorubalko, E. Gini, S. Schön, and K. Ensslin, "Measurement of Rashba and Dresselhaus Spin-orbit Magnetic Fields," Nature Phys., Vol. 3, No. 9, p. 650, 2007.

[13] B. M. Norman, C. J. Trowbridge, J. Stephens, A. C. Gossard, D. D. Awschalom, and V. Sih, "Mapping Spin-orbit Splitting in Strained (In,Ga)As Epilayers," Phys. Rev. B, Vol. 82, No. 8, p. 081304(R), 2010.

[14] S. D. Ganichev, V. V. Bel'kov, L. E. Golub, E. L. Ivchenko, P. Schneider, S. Giglberger, J. Eroms, J. De Boeck, G. Borghs, W. Wegscheider, D. Weiss, and W. Prettl, "Experimental Separation of Rashba and Dresselhaus Spin Splittings in Semiconductor Quantum Wells," Phys. Rev. Lett., Vol. 92, No. 25, p. 256601, 2004; M. Scheid, M. Kohda, Y. Kunihashi, K. Richter, and J. Nitta, "All-electrical Detection of the Relative Strength of Rashba and Dresselhaus Spin-orbit Interaction in Quantum Wires," Phys. Rev. Lett., Vol. 101, No. 26, p. 266401, 2008; M. Studer, G. Salis, K. Ensslin, D. C. Driscoll, and A. C. Gossard, "Gate-controlled Spin-orbit Interaction in a Parabolic GaAs/AlGaAs Quantum Well," Phys. Rev. Lett., Vol. 103, No. 2, p. 027201, 2009.

[15] R. Winkler, "Spin-orbit Coupling Effects in Two-dimensional Electron and Hole Systems," Springer, Berlin, 2003.

[16] Y. A. Bychkov and E. I. Rashba, "Oscillatory Effects and the Magnetic Susceptibility of Carriers in Inversion Layers," J. of Physics C: Solid State Physics, Vol. 17, No. 33, p. 6039, 1984.

[17] G. Dresselhaus, "Spin-orbit Coupling Effects in Zinc Blende Structures," Phys. Rev. Vol. 100, No. 2, pp. 580–586, 1955.

[18] G. E. Pikus and A. N. Titkov, in "Optical Orientation," edited by F. Meier and B. P. Zakharchenya, Elsevier, Amsterdam, 1984.

[19] G. C. La Rocca, N. Kim, and S. Rodriguez, "Effect of Uniaxial Stress on the Electron Spin Resonance in Zinc-blende Semiconductors," Phys. Rev. B, Vol. 38, No. 11, pp. 7595–7601, 1988.

[20] B. A. Bernevig and S.-C. Zhang, "Spin Splitting and Spin Current in Strained Bulk Semiconductors," Phys. Rev. B, Vol. 72, No. 11. p. 115204, 2005.

[21] T. Sogawa, P. V. Santos, S. K. Zhang, S. Eshlaghi, A. D. Wieck, and K. H. Ploog, "Dynamic Band-structure Modulation of Quantum Wells by Surface Acoustic Waves," Phys. Rev. B, Vol. 63, No. 12, p. 121307(R), 2001.

[22] H. Sanada, T. Sogawa, H. Gotoh, K. Onomitsu, M. Kohda, J. Nitta, and P. V. Santos, "Acoustically Induced Spin-orbit Interactions Revealed by Two-dimensional Imaging of Spin Transport in GaAs," Phys. Rev. Lett., Vol. 106, No. 21, p. 216602, 2011.

[23] S. H. Simon, "Coupling of Surface Acoustic Waves to a Two-dimensional Electron Gas," Phys. Rev. B, Vol. 54, No. 19, p. 13878, 1996.

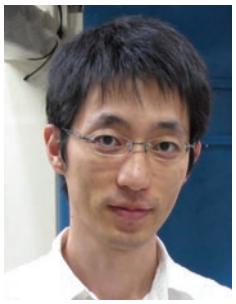

Haruki Sanada

Research Scientist, Quantum Optical Physics Research Group, Optical Science Laboratory, NTT Basic Research Laboratories.

He received the B.E., M.E., and Ph.D. degrees in electrical engineering from Tohoku University, Miyagi, in 2001, 2002, and 2005, respectively. He joined NTT Basic Research Laboratories in 2005. His research interests include the optical properties of low-dimensional semiconductor nanostructures and carrier spin dynamics modulated by surface acoustic waves and their application to solid-state quantum information processing. He is a member of the Japan Society of Applied Physics (JSAP).

Hideki Gotoh

Senior Research Scientist, NTT Basic Research Laboratories.

He received the B.E., M.E., and Ph.D. degrees in engineering from Hiroshima University in 1991, 1993, and 2000, respectively. Since joining NTT Basic Research Laboratories in 1993, he has been working on optical physics and device applications of semiconductor nanostructures. He is a member of JSAP and the Optical Society of America.

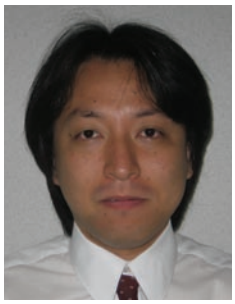

Koji Onomitsu

Research Scientist, Nanostructure Technology Research Group, Physical Science Laboratory, NTT Basic Research Laboratories.

He received the B.E. and M.E. degrees in electrical engineering from Aoyama Gakuin University, Tokyo, in 1998 and 2000, respectively, and the Ph.D. degree in electrical engineering from Waseda University, Tokyo, in 2004. He joined NTT Basic Research Laboratories in 2006. His current interests are crystal growth of modulation doped structures for high-mobility two-dimensional electron systems using MBE, mechanical devices incorporating GaMnAs, and on-chip amplifiers of mechanical vibration signals using HEMTs. He is a member of JSAP.

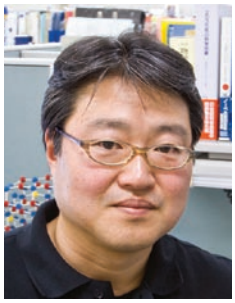

Tetsuomi Sogawa

Executive Manager of Research Planning Section, and Group Leader of Quantum Optical Physics Research Group, NTT Basic Research Laboratories.

He received the B.E., M.E., and Ph.D. degrees in electrical engineering from the University of Tokyo in 1986, 1988, and 1991, respectively. He joined NTT Basic Research Laboratories in 1991. From 2004 to 2006, he worked for the Council for Science and Technology Policy, Cabinet Office, Japan, as a deputy director for policy planning. His current research interests include fabrication technology for low-dimensional nanostructures, optical properties of quantum dots/wires and photonic crystals, spin-related phenomena, and SAW application to nanostructures. He is a member of JSAP.